Mixed Heisenberg chains: II. Thermodynamics

1998 J. Phys.: Condens. Matter 10 5217

(http://iopscience.iop.org/0953-8984/10/23/021)

J. Phys.: Condens. Matter **10** (1998) 5217–5236. Printed in the UK PII: S0953-8984(98)90481-7

Mixed Heisenberg chains: II. Thermodynamics

Harald Niggemann, Gennadi Uimin† and Johannes Zittartz

Institut für Theoretische Physik, Universität zu Köln, Zülpicher Strasse 77, D-50937 Köln, Germany

Received 7 January 1998

Abstract. We consider thermodynamic properties, e.g. specific heat and magnetic susceptibility, of alternating Heisenberg spin chains. Due to a hidden Ising symmetry, these chains can be decomposed into a set of finite chain fragments. The problem of finding the thermodynamic quantities is effectively separated into two parts. First we deal with finite objects; secondly we can incorporate the fragments into a statistical ensemble. As functions of the coupling constants, the models exhibit special features in the thermodynamic quantities, e.g. the specific heat displays double peaks at low enough temperatures. These features stem from first-order quantum phase transitions at zero temperature, which have been investigated in the first part of this work.

1. Introduction

This work is a continuation of our preceding paper [1], which is devoted to the ground-state properties of alternating Heisenberg spin chains. There we investigated 1d systems described by Hamiltonians (model A)

$$H^{(a)} = -\mathcal{J}_1 \sum_{\langle \rho, r\rangle} \boldsymbol{s}(\rho)\cdot(\boldsymbol{\sigma}(r_1)+\boldsymbol{\sigma}(r_2)) - \mathcal{J}_0 \sum_{\langle r_1, r_2\rangle} \boldsymbol{\sigma}(r_1)\cdot\boldsymbol{\sigma}(r_2) \tag{1.1}$$

or (model B)

$$H^{(b)} = -\mathcal{J}_1 \sum_{\langle \rho, r\rangle} (\boldsymbol{s}(\rho_1)+\boldsymbol{s}(\rho_2))\cdot(\boldsymbol{\sigma}(r_1)+\boldsymbol{\sigma}(r_2)) - \mathcal{J}_0' \sum_{\langle \rho_1, \rho_2\rangle} \boldsymbol{s}(\rho_1)\cdot\boldsymbol{s}(\rho_2) - \mathcal{J}_0 \sum_{\langle r_1, r_2\rangle} \boldsymbol{\sigma}(r_1)\cdot\boldsymbol{\sigma}(r_2).$$

Two kinds of lattice site, denoted by ρ and r, alternate within the chain. In both models, sites r_1 and r_2 are occupied by nearest σ-spins ($\sigma = 1/2$), which can be interpreted as forming a dumb-bell configuration perpendicular to the chain direction. r denotes their common in-chain coordinate. In model A, ρ-coordinates contain single s-spins, whereas in model B the ρ-sites are also occupied by dumbbells of s-spins with coordinates ρ_1 and ρ_2. A simple interpretation of model B is an alternating chain of orthogonal dumb-bells. In this work we concentrate on model A. However, the methods used below can be reformulated for model B as well.

Two spins, $\boldsymbol{\sigma}(r_1)$ and $\boldsymbol{\sigma}(r_2)$, are incorporated into the *compound spin* $\boldsymbol{S}(r) = \boldsymbol{\sigma}(r_1) + \boldsymbol{\sigma}(r_2)$, which is either 0, or 1. This reveals a hidden Ising symmetry of the original Heisenberg model (1.1). In fact, the $\mathcal{J}_1$ exchange term in (1.1) does not generate transitions

† On leave from: Landau Institute for Theoretical Physics, Chernogolovka, Moscow Region 142432, Russia.

0953-8984/98/235217+20$19.50

between the total spin states 0 and 1 of any compound spin. Hamiltonian (1.1) can be rewritten in a more suitable form as $H^{(a)} = H_1 + H_0^{(a)}$, where

$$H_1 = -\mathcal{J}_1 \sum_{\langle \rho, r \rangle} \boldsymbol{s}(\rho) \cdot \boldsymbol{S}(r) \tag{1.2}$$

and

$$H_0^{(a)} = -\frac{1}{2}\mathcal{J}_0 \sum_r \boldsymbol{S}^2(r). \tag{1.3}$$

$H_0^{(a)}$ counts the self-energy of a compound spin.

We can use the following obvious strategy. Any configuration of spins is characterized by intrinsic 'defects', i.e. r-sites, where the compound spin is zero. These 'defects', which are controlled by the $\mathcal{J}_0$-terms, cause the original chain to decompose into an ensemble of finite chain fragments, which are decoupled from each other. Their structure can be defined as follows. A fragment of length k ($k \geqslant 1$) is an alternating chain of $k+1$ spin-s sites and k spin-1 sites. Chain fragments are isolated from each other by a zero spin.

It is convenient to measure all energies in units of $\mathcal{J}_1$; the latter is supposed to be negative. Thus we set $\mathcal{J}_1 = -1$.

In [1] we observed successive first-order transitions governed by $\mathcal{J}_0$ at zero temperature. For model A with $s = 1/2$, it is a sequence $\langle 0 \rangle \to \langle 1 \rangle \to \langle \infty \rangle$, where a periodicity element $\langle k \rangle$ can be represented as $(s, 1)^k, s, 0$. For example, $\langle 0 \rangle$ is the periodical alternating structure, in which all r-sites are occupied by zero spins. For spins $s = 3/2$ and $s = 2$ the phase transition sequence becomes $\langle 0 \rangle \to \langle 1 \rangle \to \langle 2 \rangle \to \langle 3 \rangle \to \langle 4 \rangle \to \langle \infty \rangle$. The first two transitions, taking place at $\mathcal{J}_0^{(0,1)}$ and $\mathcal{J}_0^{(1,2)}$, are well isolated from each other, and from $\mathcal{J}_0^{(2,3)}$. The latter appears to be very close to the values of $\mathcal{J}_0^{(3,4)}$ and $\mathcal{J}_0^{(4,\infty)}$.

One appropriate method for finding and classifying all of these transitions is based on linear programming theory. For our particular problem it prescribes comparing the reduced energies

$$\frac{1}{k+1}(\epsilon_k - k\mathcal{J}_0)$$

of isolated chain fragments $(s, 1)^k, s, 0$. ϵ_k is the ground-state energy of the Hamiltonian H_1 (see (1.2)) with open boundary conditions. It is convenient to introduce the following decomposition of ϵ_k:

$$\epsilon_k = k e_\infty + e_0 + e_{\mathrm{int}}(k). \tag{1.4}$$

In (1.4) e_∞ is the energy per element $(s, 1)$ of the perfectly periodic spin structure, e_0 is the energy due to the open ends, and the remaining part, $e_{\mathrm{int}}(k)$, can be interpreted as the interaction between the chain fragment ends, which goes to zero as $k \to \infty$. Thus, *a succession of phase transitions is given by a broken line, which is concave upwards and envelops $e_{\mathrm{int}}(k)$ from below* [1]. Two typical functions $e_{\mathrm{int}}(k)$ are shown in figures 1(a) and 1(b). In the former, $e_{\mathrm{int}}(k)$ is a monotonic function, and thus the system passes through all intermediate phases from $\langle 0 \rangle$ to $\langle \infty \rangle$, when $\mathcal{J}_0$ increases from large negative values. In figure 1(b), the enveloping function corresponds to a restricted number of transitions, which is typical for mixed Heisenberg chains [1], but with increasing values of s the minimum becomes very shallow. Note that if Hamiltonian H_1 takes the form of an Ising Hamiltonian, then $e_{\mathrm{int}}(k) \equiv 0$. In a spin-wave approximation for $s \geqslant 3/2$, this function belongs to the type shown in figure 1(a).

Certainly, at non-zero temperature all phase transitions are smeared out. But thermodynamic quantities may exhibit a crucial dependence on temperature in the vicinities of

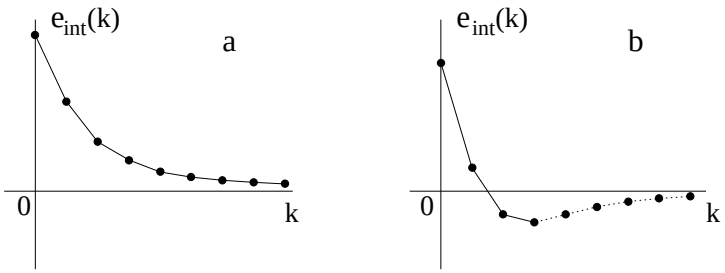

Figure 1. Two examples of possible shapes of $e_{\rm int}$ versus k: (a) represents an infinite sequence of transitions, $\langle 0\rangle \to \langle 1\rangle \to \langle 2\rangle \to \cdots \to \langle\infty\rangle$. In (b) a finite number of transitions, $\langle 0\rangle \to \langle 1\rangle \to \langle 2\rangle \to \langle 3\rangle \to \langle\infty\rangle$, is realized. The dotted part of the line does not satisfy the 'concave upwards' condition.

the critical $\mathcal{J}_0$-values. We start the next section with an example which will reveal some peculiarities of the thermodynamics of these systems.

Besides analytic methods, we have used numerical complete diagonalization of finite chain fragments. By utilizing global S^z-conservation we have been able to obtain all of the energy eigenvalues of the chain fragments with $k = 1, \ldots, 6$. The computations were performed on an Ultra Enterprise 10000 computer manufactured by Sun Microsystems. This is a parallel computer with 40 CPUs and 20 GByte of shared memory. All programs have been implemented in C++.

2. The vicinity of the $\langle 0\rangle \to \langle 1\rangle$ transition

Let us consider the vicinity of the $\langle 0\rangle \to \langle 1\rangle$ transition. For $s = 1/2$ and zero temperature the system undergoes the phase transition at $\mathcal{J}_0 = -2$. At this value the ground state is manyfold degenerate: chain fragments of unit length, $k = 1$, are embedded into the $\langle 0\rangle$ phase. This means that the distributions of 'defects' (zero spins at r-sites) is subject to the following constraint: *two 'non-defect' (spin-1) sites cannot be nearest neighbours at the r-sites. They must be separated by at least one 'defect'*. The partition function at zero temperature is the total number of all valid configurations. Let us assume that $\mathcal{Z}_n$ counts all of the configurations, which are realized between the sites $r = 0$ and $r = n$, but that the sites $r = 0$ and $r = n$ are fixed at zero spin†. This yields a recurrence relation for the partition function $\mathcal{Z}$:

$$\mathcal{Z}_n = 2\mathcal{Z}_{n-1} + \mathcal{Z}_{n-2}. \tag{2.1}$$

The two terms on the r.h.s. of (2.1) correspond to the two possibilities of $r = n - 1$ being either a 'defect' or a 'non-defect' site. If it is a 'defect' site (the first term), we count all configurations between the 'defect' sites, $r = 0$ and $r = n - 1$. The factor 2 is due to the additional spin-1/2 at the site $\rho = n - 1/2$. This spin is enclosed by 'defects', so it is *free* or paramagnetic. The second term on the r.h.s. of (2.1) corresponds to the case in which $r = n - 1$ is a 'non-defect' site. Since 'non-defects' are not allowed to be nearest neighbours, $r = n - 2$ must contain a 'defect'. Thus the configuration count of the remaining part is $\mathcal{Z}_{n-2}$. Evidently, the boundary conditions for (2.1) must be chosen as $\mathcal{Z}_0 = 1$ and $\mathcal{Z}_1 = 2$.

† We label the sites of compound spins by *integer numbers* r. For ρ, half-integers are reserved.

Now we define an additional quantity $\mathcal{D}_n$, which counts the number of 'non-defects' between the spin singlets at sites $r = 0$ and $r = n$, summed over all allowed configurations. It satisfies the equation

$$\mathcal{D}_n = 2\mathcal{D}_{n-1} + \mathcal{D}_{n-2} + \mathcal{Z}_{n-2}. \tag{2.2}$$

The first two terms on the r.h.s. of (2.2) are similar to those on the r.h.s. of equation (2.1). The third term counts how many times the 'non-defect' at $r = n - 1$ appears in all valid configurations. For $\mathcal{D}$, the boundary conditions are $\mathcal{D}_0 = 0$ and $\mathcal{D}_1 = 0$.

Let us discuss how equations (2.1) and (2.2) have to be modified in the case of non-zero temperatures. If all terms in $\mathcal{Z}_n$ are preceded by their statistical weights, we can use this quantity to calculate the partition function of a chain of length n with open boundary conditions. Instead of the set $\{\epsilon_k\}$ (cf. (1.4)), one should use the set of free energies $\{\phi_k\}$. Since we consider the vicinity of the $\langle 0\rangle \to \langle 1\rangle$ transition (i.e. $\mathcal{J}_0 \simeq -2$), only ϕ_0 and ϕ_1 enter the calculation. All other configurations are suppressed at low temperatures ($T \ll 1$). Introducing Boltzmann factors $w_k = \exp(-(\phi_k - k\mathcal{J}_0)/T)$, and setting $\phi_0 = -T\ln 2$ and $\phi_1 = -2$, we arrive at the following modification of equations (2.1) and (2.2):

$$\mathcal{Z}_n = 2\mathcal{Z}_{n-1} + w\mathcal{Z}_{n-2} \qquad w = w_1 \tag{2.3}$$

$$\mathcal{D}_n = 2\mathcal{D}_{n-1} + w(\mathcal{D}_{n-2} + \mathcal{Z}_{n-2}). \tag{2.4}$$

The solution of (2.3) is

$$\mathcal{Z}_n = c_+\lambda_+^n + c_-\lambda_-^n \qquad \lambda_\pm = 1 \pm \sqrt{1+w}.$$

For solving (2.4), we try the *ansatz*

$$\mathcal{D}_n = (a_+ + nb_+)\lambda_+^n + (a_- + nb_-)\lambda_-^n.$$

For the concentration of spin-1 sites in long chains we obtain

$$x = \lim_{n\to\infty} \frac{\mathcal{D}_n}{n\mathcal{Z}_n} = \frac{b_+}{c_+}. \tag{2.5}$$

The relationship between b_+ and c_+, which enter the leading terms of $\mathcal{D}_n$ and $\mathcal{Z}_n$ for $n \gg 1$, can be directly derived from equation (2.4):

$$\frac{b_+}{c_+} = \frac{w}{\lambda_+^2 + w} = \frac{w}{2(1 + w + \sqrt{1+w})}.$$

The physical quantities, such as the specific heat and the entropy, can straightforwardly be calculated as derivatives of the free energy. In the thermodynamic limit, i.e. for $n \to \infty$, the free energy per compound spin is simply

$$-T\ln\lambda_+ = -\frac{2+\mathcal{J}_0}{2} - \frac{T}{\sqrt{w}}$$

if $\langle 1\rangle$ is favourable ($w \gg 1$). Otherwise, for $w \ll 1$ we arrive at the expression

$$-T\ln 2 - \frac{Tw}{4}.$$

The magnetic susceptibility reflects the ground-state investigations of our former paper. In fact, as long as the chain fragments of length $k = 1$ are in the spin-singlet state, only 'isolated' spin-1/2 sites, associated with $k = 0$, contribute a Curie-like susceptibility. It can be expressed as a contribution of individual 'isolated' spins, $\mu_B^2/4T$, multiplied by their concentration

$$1 - 2b_+/c_+ = (1 + \sqrt{1+w})/(1 + w + \sqrt{1+w}).$$

This exhibits 'half-gap' behaviour, $\propto 1/\sqrt{w}$, when $w \gg 1$, i.e., $\mathcal{J}_0 > -2$. This, and the analogous w-dependence of the specific heat, can be interpreted in terms of an equilibrium chemical reaction, in which any spin singlet (1/2, 1, 1/2) may transform into *two* paramagnetic spins 1/2 and a 'defect'.

In the vicinity of the $\langle 0\rangle \to \langle 1\rangle$ transition, the results of this section are not only valid for $s = 1/2$, but also for other spins on the ρ-sites. The evident changes are as follows.

(i) $\phi_1 = -(2s+1)$, and $\mathcal{J}_0$ varies around $-(2s+1)$.
(ii) $\phi_0 = -T\ln(2s+1)$, resulting in

$$\lambda_\pm = (s+1/2) \pm \sqrt{(s+1/2)^2 + w}$$

and

$$\frac{b_+}{c_+} = \frac{w/2}{(s+1/2)^2 + w + (s+1/2)\sqrt{(s+1/2)^2+w}}.$$

(iii) A group of spins $(s, 1, s)$, whose total spin value at low temperatures is practically $(2s-1)$, is paramagnetic too, like an 'isolated' spin s.

The Curie-like susceptibility is straightforwardly calculated as

$$\frac{\mu_B^2}{3T}(2s(2s-1)b_+/c_+ + s(s+1)(1-2b_+/c_+)).$$

3. General consideration

For $s = 1/2$, quantum fluctuations are efficient enough to 'isolate' the $\langle 1\rangle \leftrightarrow \langle\infty\rangle$ transition from $\langle 0\rangle \leftrightarrow \langle 1\rangle$. In reference [1] these zero-temperature transitions were estimated as $\mathcal{J}_0^{(1,\infty)} = -0.910$ and $\mathcal{J}_0^{(0,1)} = -2$, respectively. Thus, at low temperatures we can investigate the regions around $\mathcal{J}_0^{(1,\infty)}$ and $\mathcal{J}_0^{(0,1)}$ separately. In section 2 the subject of interest is the competition of 'defect' and 'non-defect' sites, provided two 'non-defects' cannot be nearest neighbours, if $\mathcal{J}_0$ is around $\mathcal{J}_0^{(0,1)}$. On the other hand, two 'defects' cannot be nearest neighbours in the second critical range around $\mathcal{J}_0^{(1,\infty)}$ at low temperatures. Instead of dealing with 'defect' and 'non-defect' objects, let us use the convention of reference [1]. For convenience, chain fragments have been defined as follows. A chain fragment of length k formally includes a spin-0 site from its right, so it can be represented as $(1/2, 1)^k(1/2, 0)$. Conventionally, the nearest spin from the left of any chain fragment is also 0, but this spin is incorporated into the fragment which lies on the l.h.s. of this site. In this classification, (1/2, 0) is a chain fragment of zero length.

Now we can reformulate one of the statements mentioned above. In the second 'critical' range around $\mathcal{J}_0^{(1,\infty)}$, zero-length chain fragments are uncompetitive and may be neglected at low temperatures. However, we shall see from the specific heat calculation that at intermediate temperatures, e.g. $T = 0.3$, and for $\mathcal{J}_0$ intermediate between $\mathcal{J}_0^{(0,1)}$ and $\mathcal{J}_0^{(1,\infty)}$, not only do chain fragments of unit length dictate thermodynamic properties, but also longer chain fragments and zero-length fragments contribute significantly. Therefore we have to take into account chain fragments of any length, and no special restrictions on the values of $\mathcal{J}_0$ and temperature will be imposed.

The free energy of a chain fragment of length k can be written as a generalization of equation (1.4):

$$\phi_k = kf_\infty + f_0 + f_{\rm int}(k) \tag{3.1}$$

where f_∞, f_0, and $f_{\rm int}$ are temperature dependent. In this section, the configurational part of the free energy will be determined by making use of recursive relations similar to (2.3) and (2.4).

It is convenient to take the global configuration $\langle\infty\rangle$ as the 'vacuum' state. A zero spin within this background is called a 'hole'. If we ignore the interaction term in (3.1), i.e. $f_{\rm int}(k)$, then any 'hole' costs the free energy $(\mathcal{J}_0 - f_\infty(T)) + f_0(T)$. In fact, the free energy of a very long chain, $nf_\infty(T) + f_0(T)$, becomes $(n-1)f_\infty(T) + 2f_0(T) + \mathcal{J}_0$ if a 'hole' is inserted. For two 'holes' we obtain $(n-2)f_\infty(T) + 3f_0(T) + 2\mathcal{J}_0$, and so on. However, this consideration is no longer valid if two 'holes' occupy nearest-neighbour sites on the r-sublattice. Two such 'holes' give rise to a zero-length chain fragment. In this case we obtain $(n-2)f_\infty(T) + 2f_0(T) + 2\mathcal{J}_0$, which can be subdivided into $(n-1)f_\infty(T) + 2f_0(T) + \mathcal{J}_0$ and $-f_\infty(T)\mathcal{J}_0$. The latter should be interpreted as the free energy of the zero-length chain fragment. Only the 'holes' which are separated by a chain fragment of non-zero length and which do not have other 'holes' between them, interact via $f_{\rm int}(k;T)$, where $k \geqslant 1$ is the chain fragment length, or the number of spin-1 sites between these *nearest* holes. We denote the statistical weight of a chain fragment of length k by w_k. Then starting with

$$w_0 = \exp\left[-(\mathcal{J}_0 - f_\infty)/T\right] \qquad \text{and} \qquad w_1 = \exp\left[-(\mathcal{J}_0 - f_\infty + f_0 + f_{\rm int}(1))/T\right]$$

we obtain

$$w_k = w_1 \exp\left[(f_{\rm int}(1) - f_{\rm int}(k))/T\right] \qquad k \geqslant 1 \tag{3.2}$$

for longer chain fragments.

The recurrence relations for the partition function are obvious generalizations of (2.3):

$$\mathcal{Z}_{n+1} = 2w_0\mathcal{Z}_n + w_1\mathcal{Z}_{n-1} + w_2\mathcal{Z}_{n-2} + \cdots + w_k\mathcal{Z}_{n-k} + \cdots + w_n\mathcal{Z}_0 \qquad n \geqslant 1. \tag{3.3}$$

Each $\mathcal{Z}_k$ counts all possible spin configurations with corresponding statistical weights between $r = 0$ and $r = k$, while fixing the boundary compound spins at $r = 0$ and $r = k$ at zero. The prefactor 2 of $w_0\mathcal{Z}_n$ on the r.h.s. of equation (3.3) is due to the spin-1/2 at site $\rho = n + 1/2$. The boundary conditions for the set of partition functions are $\mathcal{Z}_0 = 1$ and $\mathcal{Z}_1 = 2w_0$. The latter reflects the existence of a free spin-1/2 between two spin-0 sites.

The lower index in $\mathcal{D}_k^{(m)}$ has the same meaning as in $\mathcal{Z}_k$, whereas the upper index is related to the chain fragment length. $\mathcal{D}_k^{(m)}$ measures how often chain fragments of length m occur between the sites $r = 0$ and $r = k$. Of course, any spin configuration in $\mathcal{D}_k^{(m)}$ picks up a corresponding statistical weight. The recurrence relations for the shortest chain fragments, $k = 0$ and 1, have a structure which is similar to that of equation (3.3):

$$\mathcal{D}_{n+1}^{(0)} = 2w_0\mathcal{Z}_n + 2w_0\mathcal{D}_n^{(0)} + w_1\mathcal{D}_{n-1}^{(0)} + \cdots + w_k\mathcal{D}_{n-k}^{(0)} + \cdots + w_n\mathcal{D}_0^{(0)} \qquad n \geqslant 1. \tag{3.4}$$

$$\mathcal{D}_{n+1}^{(1)} = w_1\mathcal{Z}_{n-1} + 2w_0\mathcal{D}_n^{(1)} + w_1\mathcal{D}_{n-1}^{(1)} + \cdots + w_k\mathcal{D}_{n-k}^{(1)} + \cdots + w_n\mathcal{D}_0^{(1)} \qquad n \geqslant 1. \tag{3.5}$$

The first terms on the r.h.s. of (3.4) and (3.5) are the contributions of the spin-0 and spin-1 sites at $r = n$, respectively. The boundary condition, which should be imposed on $\mathcal{D}^{(0)}$, reads $\mathcal{D}_0^{(0)} = 0$. For $\mathcal{D}^{(1)}$, we can set $\mathcal{D}_0^{(1)} = 0$ and $\mathcal{D}_1^{(1)} = 0$.

The generalization of the recurrence relations and boundary conditions to arbitrary chain fragment lengths m is also obvious:

$$\begin{aligned} \mathcal{D}_{n+1}^{(m)} &= w_m\mathcal{Z}_{n-m} + 2w_0\mathcal{D}_n^{(m)} + w_1\mathcal{D}_{n-1}^{(m)} \\ &\quad + \cdots + w_k\mathcal{D}_{n-k}^{(m)} + \cdots + w_n\mathcal{D}_0^{(m)} \qquad \text{for } n \geqslant m \\ \mathcal{D}_n^{(m)} &= 0 \qquad\qquad \text{for } n \leqslant m. \end{aligned} \tag{3.6}$$

We define the concentration x_m of chain fragments of length m as the ratio of the expectation value of their total number $N_m = \mathcal{D}_n^{(m)}/\mathcal{Z}_n$ to the total number of r-sites, n:

$$x_m = \lim_{n\to\infty} \frac{\mathcal{D}_n^{(m)}}{n\mathcal{Z}_n} \tag{3.7}$$

which is similar to equation (2.5). These concentrations must satisfy the conservation law

$$1 = \sum_{k\geqslant 0}(k+1)x_k \tag{3.8}$$

which states that the total number of compound spins, zeros and ones, is equal to the total number of r-sublattice sites.

The set of equations (3.3)–(3.6) allows us to perform a straightforward numerical analysis. However, let us try an analytical approach by assuming that $|f_{\rm int}(k) - f_{\rm int}(1)| \ll T$ for all $k \geqslant 1$. Practically, this means that

$$T \gg |f_{\rm int}(1)| \tag{3.9}$$

which is well satisfied at $T > 0.15$, as we shall see in section 4. In this approximation one can set $w_k = w$ for all $k \geqslant 1$. By subtracting $\mathcal{Z}_n$ from $\mathcal{Z}_{n+1}$, we can rewrite equations (3.3) in a simple form ($n \geqslant 1$):

$$\mathcal{Z}_{n+1} - (1+2w_0)\mathcal{Z}_n + (2w_0 - w_1)\mathcal{Z}_{n-1} = 0. \tag{3.10}$$

The analogous equations for $\mathcal{D}_k^{(0)}$ and $\mathcal{D}_k^{(1)}$ are similar, but have different r.h.s. and boundary conditions:

$$\mathcal{D}_{n+1}^{(0)} - (1+2w_0)\mathcal{D}_n^{(0)} + (2w_0 - w_1)\mathcal{D}_{n-1}^{(0)} = 2w_0(\mathcal{Z}_n - \mathcal{Z}_{n-1}) \qquad n \geqslant 1$$
$$\mathcal{D}_0^{(0)} = 0 \qquad \mathcal{D}_1^{(0)} = 2w_0. \tag{3.11}$$

$$\mathcal{D}_{n+1}^{(1)} - (1+2w_0)\mathcal{D}_n^{(1)} + (2w_0 - w_1)\mathcal{D}_{n-1}^{(1)} = w_1(\mathcal{Z}_{n-1} - \mathcal{Z}_{n-2}) \qquad n \geqslant 2$$
$$\mathcal{D}_0^{(1)} = \mathcal{D}_1^{(1)} = 0 \qquad \mathcal{D}_2^{(1)} = w_1. \tag{3.12}$$

As in the case of equations (2.3) and (2.4), we look for solutions $\mathcal{Z}_n$, $\mathcal{D}_n^{(0)}$, and $\mathcal{D}_n^{(1)}$ of the form

$$c_+\lambda_+^n + c_-\lambda_-^n$$
$$(a_+ + b_+^{(0)}n)\lambda_+^n + (a_- + b_-^{(0)}n)\lambda_-^n$$

and

$$(a_+ + b_+^{(1)}n)\lambda_+^n + (a_- + b_-^{(1)}n)\lambda_-^n$$

respectively. By inserting this *ansatz* we obtain

$$\lambda_+ = w_0 + 1/2 + \sqrt{2w_0^2 + w_1 + 1/4}$$

and the concentrations of chain fragments of length $k = 1$ and 0:

$$x_1 = \frac{b_+^{(1)}}{c_+} = \frac{w_1(\lambda_+ - 1)}{\lambda_+(\lambda_+^2 + w_1 - 2w_0)} \tag{3.13}$$

$$x_0 = \frac{b_+^{(1)}}{c_+} = \frac{2w_0\lambda_+}{w_1}x_1. \tag{3.14}$$

Generalization of equation (3.13) for $m > 1$ is straightforward: the analogue of (3.12) now reads

$$\mathcal{D}_{n+1}^{(m)} - (1+2w_0)\mathcal{D}_n^{(m)} + (2w_0 - w_1)\mathcal{D}_{n-1}^{(m)} = w_1(\mathcal{Z}_{n-m} - \mathcal{Z}_{n-m-1}) \qquad n \geqslant m+1 \tag{3.15}$$

while the boundary conditions can be written as

$$\mathcal{D}_0^{(m)} = \cdots = \mathcal{D}_m^{(m)} = 0 \qquad \mathcal{D}_{m+1}^{(m)} = w_1.$$

The above-mentioned asymptotic behaviour of $\mathcal{Z}_n$ and $\mathcal{D}_n^{(m)}$ allows us to determine the concentration x_m as

$$x_m = \frac{b_+^{(m)}}{c_+} = \frac{1}{(\lambda_+)^{m-1}} x_1. \tag{3.16}$$

It is not difficult to check the validity of the sum rule (3.8) with equations (3.14), (3.13), and (3.16).

Just comparing two sets of equations, (3.12) and (3.15), one can conclude that the knowledge of all $\mathcal{D}_k^{(1)}$ allows us to calculate any expression of higher rank, e.g.

$$\mathcal{D}_{n+m-1}^{(m)} = \mathcal{D}_n^{(1)}. \tag{3.17}$$

At lower temperatures it is necessary to bring in more Boltzmann factors. The simplest extension of the temperature range

$$T \gg |f_{\text{int}}(2)| \tag{3.18}$$

does not impose restrictions on $|f_{\text{int}}(1)|$ any longer; the latter is not necessarily much smaller than the temperature. This leads us to the introduction of three Boltzmann factors, w_0, w_1, and $w_k = w_2 \approx w_1 \exp[f_{\text{int}}(1)/T]$, if $k \geqslant 2$ (see definition (3.2)). The numerical results given in the next section will show that such a description is a good approximation for $T > 0.04$. This is a systematic way to extend our approach to lower temperatures. By using four Boltzmann factors, the system can be described down to $T \approx 0.01$.

In appendix A we outline how the method developed above works in the general situation, where temperature is restricted from below: $T \gg |f_{\text{int}}(k)|$. In this case we deal with a set of statistical weights

$$\{w_0, w_1, w_2, \ldots, w_{k-1}, w_n = w_k (n \geqslant k)\}. \tag{3.19}$$

4. Numerical computations

4.1. Chain fragments: zero-field results

By using complete matrix diagonalization we have computed all of the energy eigenvalues of finite chain fragments up to $k = 6$. From these eigenvalues, the exact values of the free energy for various temperatures have been calculated. We decompose the free energy into an affine contribution $kf_\infty + f_0$ and an 'interaction' contribution $f_{\text{int}}(k)$. This decomposition is defined by

$$\lim_{k\to\infty} f_{\text{int}}(k) = 0.$$

Table 1 shows computed values of $f_{\text{int}}(k)$ for $T = 0.02$, $T = 0.3$, and $T = 1.0$. Free-energy values for $k = 5$ and $k = 6$ have been used to determine f_0 and f_∞, so

$$f_{\text{int}}(5) = f_{\text{int}}(6) \equiv 0$$

for all temperatures. The accuracy of this approximation can be estimated from figures 2, 3, and 4, where $f_{\text{int}}(k)$ decays quickly and smoothly to zero.

For low temperatures ($T < 0.3$), the k-dependence of the free energy is qualitatively similar to the ground-state energy. This is illustrated in figure 2. As in the ground-state energy, there is a clear minimum at $k = 1$, which corresponds to the phase transition sequence $\langle 0\rangle \to \langle 1\rangle \to \langle \infty\rangle$ at $T = 0$.

Table 1. The 'interaction' contribution $f_{\rm int}(k)$ of the free energy for $T = 0.02$, $T = 0.3$, and $T = 1.0$.

k	$T = 0.02$	$T = 0.3$	$T = 1.0$
0	0.454 050	0.245 974	0.027 743
1	−0.074 381	0.002 104	0.000 148
2	−0.012 040	$-9.540\,148 \times 10^{-5}$	$8.060\,468 \times 10^{-7}$
3	−0.000 113	$-5.336\,452 \times 10^{-6}$	$4.404\,270 \times 10^{-9}$
4	0.000 476	$-8.747\,215 \times 10^{-8}$	$2.376\,055 \times 10^{-11}$
5	0.0	0.0	0.0
6	0.0	0.0	0.0

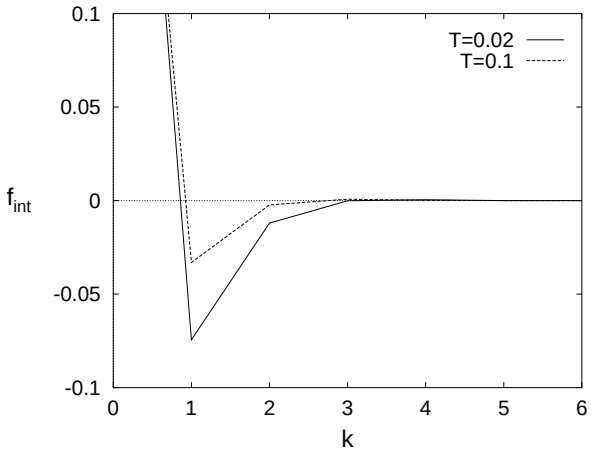

Figure 2. The computed free energy versus k after subtracting the affine contribution $kf_\infty + f_0$ for low temperatures $T = 0.02$ (full line) and $T = 0.1$ (dashed line)

For $T > 0.3$, the increase in temperature has led to the ground-state structure being completely smeared out. Deviations from the affine contribution $kf_\infty + f_0$ decay exponentially as a function of k. This is shown in figure 3 for $T = 0.5$ and $T = 1.0$.

In the crossover region where $T \simeq 0.3$, we observe an interesting phenomenon: as shown in figure 4, the minimum of the free energy has moved from $k = 1$ to $k = 2$. This is due to the spin degeneracy of the chain fragment. The total spin of a chain fragment of length k is $s_p = (k - 1)/2$ for low temperatures, so the degeneracy is $2s_p + 1 = k$. This yields

$$f_{\rm deg} = -T \ln k$$

as an additional contribution to the free energy. If we subtract this additional contribution from $f_{\rm int}$, the minimum at $k = 1$ is restored. This contribution is *only* relevant at intermediate temperatures: at low temperatures it is suppressed by the prefactor T; at high temperatures the $\ln k$ contribution to the spin entropy is no more dominant. Indeed, the magnetic behaviour of short chain fragments cannot be described by a single paramagnetic spin s_p. In other words, at high temperatures the spin–spin correlation length becomes smaller than k.

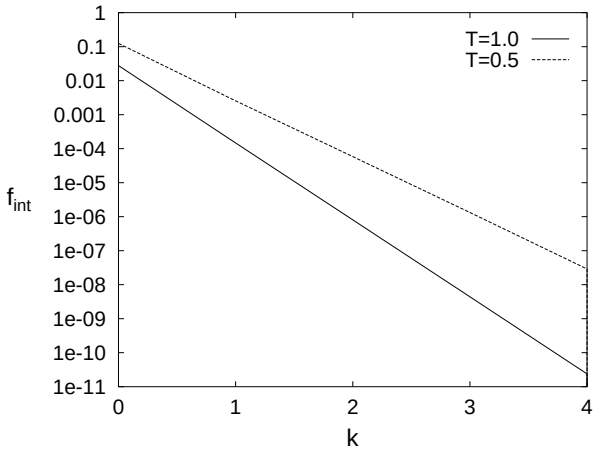

Figure 3. The 'interaction part' of the free energy as a function of k for high temperatures $T = 1.0$ (full line) and $T = 0.5$ (dashed line)

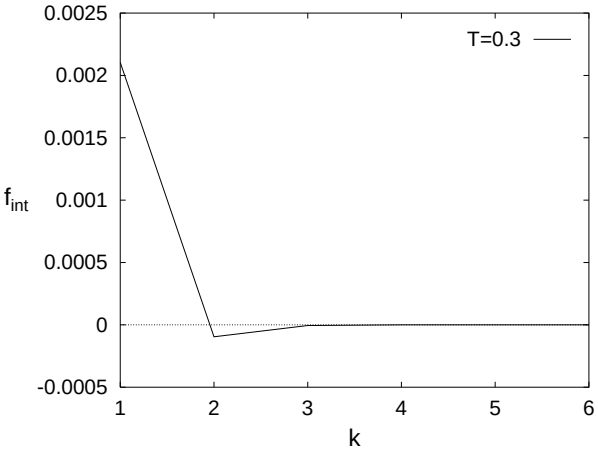

Figure 4. The 'interaction part' of the free energy as a function of k at the crossover temperature $T_c \simeq 0.3$.

4.2. Chain fragments: magnetic susceptibility

By including small magnetic fields in the Hamiltonian, we have computed the zero-field susceptibility for $k = 1, \ldots, 5$ and various temperatures.

There are two contributions to the magnetic susceptibility.

(i) The paramagnetic contribution, which is

$$\chi_p = \frac{1}{3T} s_p(s_p + 1) \tag{4.1}$$

for low temperatures.

(ii) The contribution χ_a due to the antiferromagnetic correlations inside the chain fragment. Though the exact form of this contribution is unknown, it is expected to be approximately linear in k and only slowly varying as a function of temperature.

Figure 5 shows the magnetic susceptibility as a function of inverse temperature for fragment lengths $k = 2, \ldots, 5$. The numerically computed values (various symbols) are almost perfectly connected by the exactly known paramagnetic contribution (4.1) (lines), where $(k-1)/2$ has been inserted for s_p. Please note that there are no fit parameters.

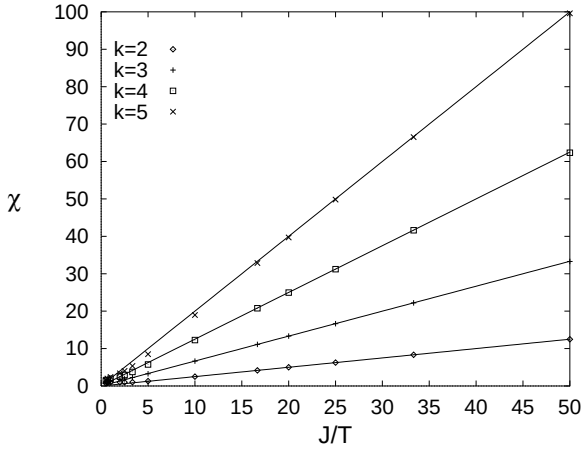

Figure 5. The computed magnetic susceptibility for $k = 2, \ldots, 5$ (symbols) and the paramagnetic contribution (4.1) (lines)

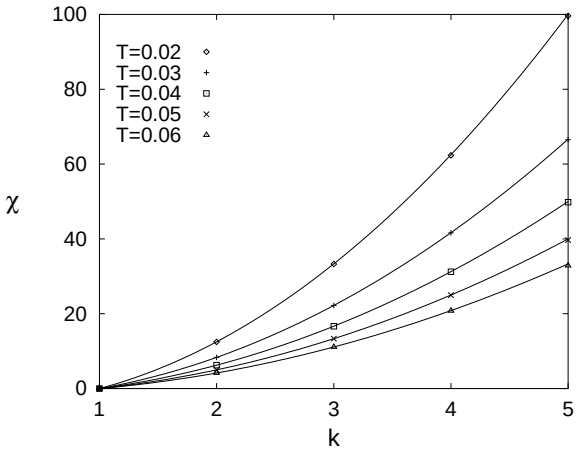

Figure 6. The computed magnetic susceptibility for $T = 0.02, \ldots, 0.06$ (symbols) and the paramagnetic contribution (4.1) (lines)

Therefore, at least for low temperatures, the susceptibility is well described by the Curie law (4.1). For higher temperatures, χ_p is not strictly linear in T^{-1}. Additionally, with increasing temperature the antiferromagnetic contribution χ_a decays more slowly than χ_p, so χ_a may become relevant for larger T.

Of course, the coincidence of χ with χ_p for low temperatures can also be observed when plotting χ as a function of the fragment length k. This is shown in figure 6 for temperatures $0.02 \leqslant T \leqslant 0.06$.

For high temperatures, the correlation length becomes smaller than the fragment length.

In this case, the effective total spin can be interpreted as being composed of several independent blocks of individual spins. The typical length of these blocks is the correlation length ξ, so the effective total spin square $s_p(s_p+1)$ is proportional to ξk, in contrast to the low-temperature situation, where $s_p = (k-1)/2$. This results in a *linear* χ versus k dependence, which is numerically confirmed, as shown in figure 7. There we have successfully fitted affine functions

$$\chi_h = a_0(T) + a_1(T)k \tag{4.2}$$

to the computed data points.

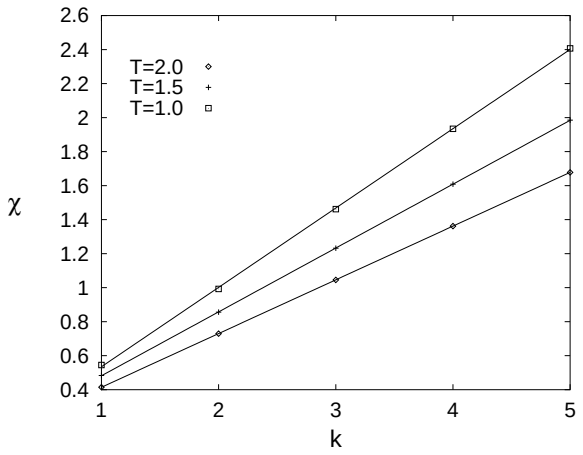

Figure 7. The computed magnetic susceptibility for $T = 1.0, 1.5, 2.0$ (symbols) and fitted affine functions (4.2) (lines)

If we were to extend figure 6 to large values of k, we would certainly observe a crossover from a parabolic to a linear k-dependence at sufficiently large fragment length k. The crossover region depends on the temperature.

We finish this section by considering intermediate temperatures, for which the crossover behaviour can be observed at finite fragment length $k < 6$. Figure 8 shows this intermediate-temperature region. The crossover from quadratic to linear behaviour is governed by a logarithmic correction

$$\chi_i = b_0(T_i) + b_1(T_i)k + b_2(T_i)\ln k \tag{4.3}$$

which fits $\chi(k)$ successfully for temperatures around $T = 0.3$. This behaviour is presumably reminiscent of the crossover in the free energy, which takes place at the same temperature range.

4.3. Mixed chains as ensembles of chain fragments

This part of the paper is a kind of synthesis of the analytic approach developed in section 3 and the numerical computations performed in section 4. We shall illustrate this by computing the specific heat for two temperatures, low and intermediate, $T = 0.02$ and $T = 0.3$, and for reasons which will be explained below, the magnetic susceptibility versus $\mathcal{J}_0$ will be calculated for intermediate temperatures $T = 0.1$ and $T = 0.3$. Please note that in section 2 we derived an analytical expression for the magnetic susceptibility, which holds in the

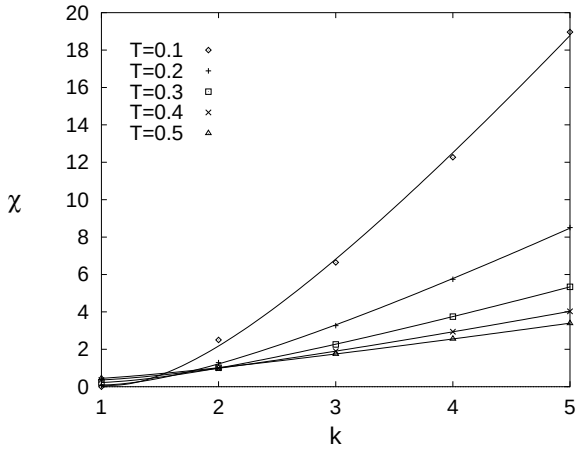

Figure 8. The computed magnetic susceptibility for intermediate temperatures (symbols) and fitted functions (4.3) (lines)

vicinity of the $\langle 0\rangle \to \langle 1\rangle$ transition, where all contributions of chain fragments of length $k \geqslant 2$ can be neglected, i.e. at low enough temperatures.

The specific heat per compound spin is calculated as

$$C = -T\frac{\partial^2 f}{\partial T^2}$$

where f is the total free energy of the alternating chain. In the thermodynamic limit, the partition function is given by the logarithm of the maximum root $\lambda_{\max}$ of the polynomial (A.3). The 'reference state' in the derivation of the partition function is the perfect $\langle\infty\rangle$-structure, so the complete free energy is given by

$$f = -T\ln(\lambda_{\max}) + f_\infty. \tag{4.4}$$

According to table 1 we have the estimate

$$|f_{\rm int}(k)| \ll 0.02 \qquad \text{for } k \geqslant 3.$$

Therefore it is sufficient to work with four different Boltzmann weights, $w_0, \ldots, w_3$. (At $T = 0.3$, this approximation is even more accurate.) The polynomial (A.3) specializes to

$$\lambda^4 - (1 + 2w_0)\lambda^3 + (2w_0 - w_1)\lambda^2 + (w_1 - w_2)\lambda + (w_2 - w_3) = 0.$$

Values for f_∞ and $w_0, \ldots, w_3$ have been obtained from the numerical results outlined in subsection 4.1.

Figure 9 shows the resulting specific heat as a function of $\mathcal{J}_0$ for $T = 0.02$. As expected, the most interesting features can be found in the regions around $\mathcal{J}_0^{(0,1)}$ and $\mathcal{J}_0^{(1,\infty)}$. In order to understand the double-peak structure, which is shown in the inset, consider the expression

$$f(T) = \sum_{k\geqslant 0} x_k(T)\phi_k(T)$$

for the total free energy of the alternating chain. As indicated, both the concentrations x_k and the free energies ϕ_k of the finite fragments depend on temperature, so the specific heat involves x_k itself and its first and second derivatives. At low temperatures, x_k is a step-like function, which qualitatively explains the splittings of the peaks and their shapes.

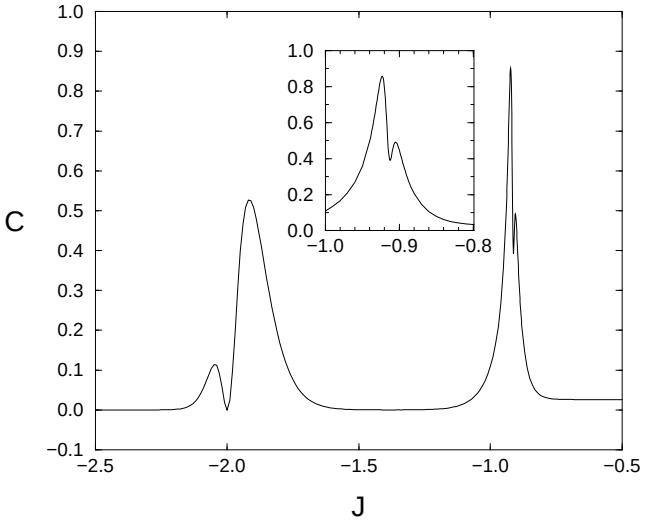

Figure 9. The specific heat of the full alternating chain as a function of $\mathcal{J}_0$ at $T = 0.02$. The inset shows the fine double-peak structure at around $\mathcal{J}_0^{(1,\infty)}$. Note that for $\mathcal{J}_0 > -0.7$ the specific heat approaches a non-zero value (temperature dependent!), which is the specific heat of the perfect alternating chain $\cdots$–1/2–1–1/2–1–$\cdots$.

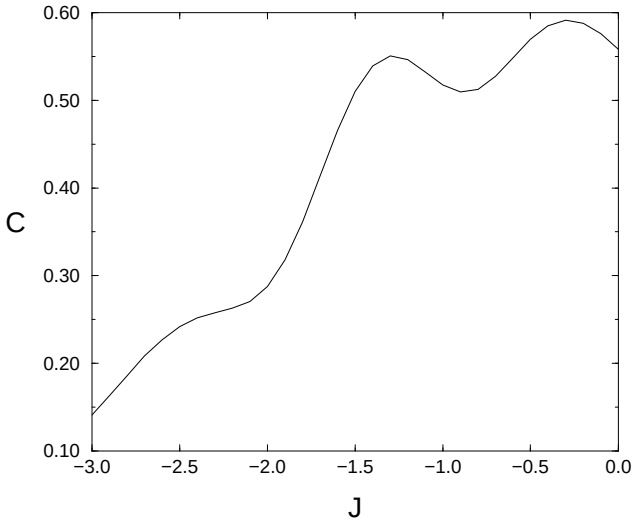

Figure 10. The specific heat of the full alternating chain as a function of $\mathcal{J}_0$ at $T = 0.3$. It decays to zero for large negative $\mathcal{J}_0$; e.g. $C \approx 0.02$ at $\mathcal{J}_0 = -4$.

At $T = 0.3$, the increase in temperature has led to the fine structure at around $\mathcal{J}_0^{(0,1)}$ and $\mathcal{J}_0^{(1,\infty)}$ being smeared out. The two regions are not isolated from each other; nevertheless the double-peak structure is still visible in figure 10.

Figures 9 and 10 illustrate the dependence of the specific heat on the interior coupling constant $\mathcal{J}_0$. The temperature dependence of C will be published in future work.

Calculation of the magnetic susceptibility per compound spin is straightforward. It is

simply given by

$$\chi = \sum_{k \geqslant 0} x_k \chi_k \tag{4.5}$$

where χ_k is the susceptibility of a finite chain fragment of length k. The concentrations x_k according to (A.8) and (A.10) are computed by specializing to just four different Boltzmann weights. χ_0 is the susceptibility of an isolated paramagnetic spin-1/2. In units of μ_B^2, $\chi_0 = 1/4T$. $\chi_1, \ldots, \chi_5$ are known numerically from subsection 4.1. For $\mathcal{J}_0 < \mathcal{J}_0^{(1,\infty)}$ the largest eigenvalue $\lambda_{\max} \gg 1$, so because of (A.10) we can safely cut off the summation (4.5) after $k = 5$. As $\mathcal{J}_0$ approaches $\mathcal{J}_0^{(1,\infty)}$, all concentrations x_k for finite k quickly decay to zero, as $\langle\infty\rangle$ becomes the dominating configuration. The susceptibility χ_∞ of this configuration is unknown for $T = 0.02$, but we can extrapolate it easily for those temperatures for which χ versus k is in the linear regime. From the calculations performed in subsection 4.2, χ_∞ per compound spin can be estimated as follows:

$$\begin{aligned} T = 0.1: &\qquad \chi' = \lim_{k\to\infty} \frac{1}{k}\chi_k \approx 6.70 \\ T = 0.3: &\qquad \chi' = \lim_{k\to\infty} \frac{1}{k}\chi_k \approx 1.60. \end{aligned} \tag{4.6}$$

Unfortunately, the convergence of the series (4.5) is very bad if $\mathcal{J}_0 > \mathcal{J}_0^{(1,\infty)}$. At intermediate temperatures, this problem can be circumvented by making use of the sum rule (3.8) and the relations

$$\begin{aligned} &\lambda_{\max} \to 1 && \text{for increasing } \mathcal{J}_0 \\ &x_k \propto \lambda_{\max}^{-k} && \text{for large } k \\ &\chi_k \propto k && \text{for large } k. \end{aligned}$$

This procedure is illustrated in appendix B. However, in order to obtain reasonable results one needs to know the whole set of χ_k before the k-dependence becomes linear. There is no problem in the cases of temperatures $T = 0.3$ and $T = 0.1$ (cf. figure 8), but the set of χ_k at $T = 0.02$ is too far from the linear regime (see figure 6).

In figures 11 and 12, which show the magnetic susceptibility for $T = 0.1$ and $T = 0.3$, we have used figure 8 as a prerequisite, i.e. we extracted the fragment susceptibilities $\chi_0, \ldots, \chi_5$, and the asymptotic slope χ'. Figures 11 and 12 have the correct asymptotics: at large negative $\mathcal{J}_0$ the susceptibility approaches $1/(4T)$, while at large positive $\mathcal{J}_0$ it is in accordance with (4.6).

5. Summary and forward look

In this work we have combined analytical and numerical methods for calculating thermodynamical properties of alternating Heisenberg chains. Interest in these spin systems is not purely academic. In fact, recent progress in the observation of quantum effects for quasi-one-dimensional antiferromagnets (see e.g. [2] and [3]) has been commonly made by physicists and crystal growth experts. It is outside the scope of the present work to recommend some specific compounds which might be good candidates for exhibiting mixed chains with such a competitive behaviour. Schematically, their simplest representation is given in our description with models A and B (see also the illustrations in [1]).

It should be emphasized that the unusual thermodynamic behaviour described in this paper can be efficiently observed in those compounds for which the values of the coupling

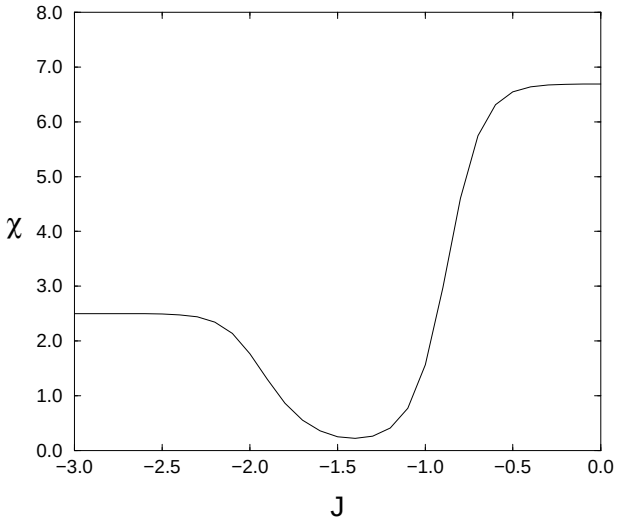

Figure 11. The magnetic susceptibility of the full alternating chain as a function of $\mathcal{J}_0$ at $T = 0.1$.

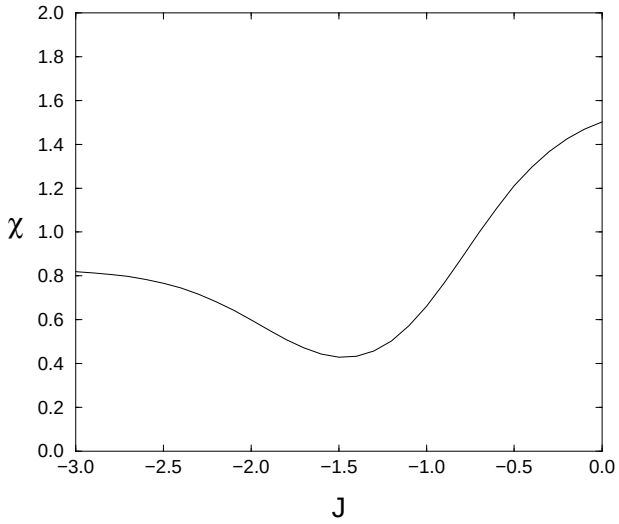

Figure 12. The magnetic susceptibility of the full alternating chain as a function of $\mathcal{J}_0$ at $T = 0.3$.

constants J_0 and J_1 lead to competitive interactions. Then a major contribution to the thermodynamic quantities comes from thermal changes of the fragment concentrations x_k.

(i) To make the basic ideas transparent, we employ a simple representation of these chains: 'compound spins' and spin-1/2 sites alternate within the chain. They interact via a coupling constant $\mathcal{J}_1$. A compound spin consists of two spin-1/2 sites forming a dumb-bell configuration perpendicular to the chain direction. The constituents of a dumb-bell interact via the internal coupling constant $\mathcal{J}_0$. The intrinsic state of a compound spin is either spin-1 or spin-0, which gives rise to the hidden Ising symmetry of the Heisenberg

chain. Spin-0 states can be treated as 'defects' with respect to the perfect alternating chain $\cdots$–1/2–1–1/2–1–$\cdots$. These equilibrium 'defects' simply break the perfect chain into a set of non-interacting chain fragments of finite lengths, whose general formula is $(\frac{1}{2}, 1)^k \frac{1}{2}$ for length $k \geqslant 0$.

(ii) At zero temperature, one of three ground states is realized, depending on the value of $\mathcal{J}_0$ ($\mathcal{J}_1$, the antiferromagnetic exchange, is set to -1): $\langle 0 \rangle$, the regular structure of chain fragments of length $k = 0$ for $\mathcal{J}_0 < -2$—this means that all compound spins are zero; $\langle 1 \rangle$, the regular structure of chain fragments of length $k = 1$ for $-2 < \mathcal{J}_0 < -0.910$—i.e. compound spins 0 and 1 alternate with each other; $\langle \infty \rangle$, there is only one 'fragment' of infinite length for $-0.910 < \mathcal{J}_0$—i.e. all compound spins are 1. Although the first-order transitions governed by $\mathcal{J}_0$ are smeared out at non-zero temperature, thermodynamic quantities display a strong dependence on $\mathcal{J}_0$ and temperature in the vicinities of the zero-temperature critical values.

(iii) As a function of $\mathcal{J}_0$, the specific heat displays two peaks, which are reminiscent of the zero-temperature transitions $\langle 0 \rangle \to \langle 1 \rangle \to \langle \infty \rangle$. As shown in figure 9, these peaks are split at low temperatures. The origin of this fine structure is the step-like behaviour of the fragment concentrations x_k, predominantly x_0 and x_1. With increasing temperature, the peaks become broader and overlap, but the local minima still indicate the vicinities of the critical $\mathcal{J}_0$-values; cf. figure 10. The crucial dependence of the magnetic susceptibility on $\mathcal{J}_0$ and T is illustrated in figures 11 and 12. Technically it is more difficult to compute $\chi(\mathcal{J}_0)$ because of the poor convergence of the series (4.5). We have eliminated these difficulties by making use of the sum rule (3.8).

(iv) All these pretransitional phenomena, which can be identified clearly, are provided by the configurational contributions to thermodynamic quantities. We have developed an analytic approach for calculating the free energy and the concentrations of chain fragments of different lengths. This is achieved by solving polynomial equations, whose degree increases at lower temperature. In fact, the hierarchical structure of the equations is regulated by $f_{\mathrm{int}}(k)$, i.e. the part of the free energy of a chain fragment of length k which can be interpreted as the interaction of fragment ends. From numerical computations we observed that f_{int} decays rapidly with k.

(v) For other alternating chains, in which the non-compound sites are occupied by higher spins s instead of 1/2, there are several successive zero-temperature transitions with increasing $\mathcal{J}_0$. The last one is $\langle 4 \rangle \to \langle \infty \rangle$ which occurs if $s \geqslant 3/2$. For these chains, the occurrence of several peaks in the specific heat would be possible. However, very low temperatures are needed to isolate some peaks: although the successive transitions $\langle 0 \rangle \to \langle 1 \rangle$ and $\langle 1 \rangle \to \langle 2 \rangle$ are sufficiently separated, the distance between the transitions $\langle 3 \rangle \to \langle 4 \rangle$ and $\langle 4 \rangle \to \langle \infty \rangle$ is only $\Delta\mathcal{J}_0 \sim 10^{-3}$.

(vi) To investigate the thermodynamics of alternating chains with $s > 1/2$, other methods could be used instead of exact numerical diagonalization. A modification of the spin-wave approximation, which can be adjusted to our problem, has been proposed by Takahashi [4]. In [5] and [6], the quantum transfer matrix of exactly solvable spin chains has been investigated in order to calculate thermodynamic quantities. A combination of this approach and numerical methods could be applied to our problem.

(vii) Generalization to higher dimensions is straightforward: for instance in two dimensions, the 'white' squares of a chequerboard lattice contain single spins, while the 'black' ones are occupied by compound spins. Competition may again reveal a hidden Ising-like variable and possible two-dimensional superstructures. Of course, similar models can be constructed on any bipartite lattice.

Acknowledgment

This work was performed within the research programme of the Sonderforschungsbereich 341, Köln–Aachen–Jülich.

Appendix A

As shown in section 4, $f_{\rm int}(k)$ decays rapidly at high temperatures. But even at very low temperatures, $T = 0.02$, we have the estimate

$$|f_{\rm int}(k)| \ll T \qquad \text{for } k \geqslant 3.$$

According to the method developed in section 3, it is sufficient to introduce the set of Boltzmann weights:

$$\{w_1, w_2 = w_1 \exp[(f_{\rm int}(1) - f_{\rm int}(2))/T], w_3 = w_1 \exp[f_{\rm int}(1)/T], w_n = w_3 (n \geqslant 3)\}.$$

In this appendix we outline the procedure for the general case, where all statistical weights (3.19) are taken into account.

If we substitute $n - 1$ for n in (3.3) and subtract the resulting expression from the original equation (3.3) we arrive at

$$\mathcal{Z}_{n+1} - (1 + 2w_0)\mathcal{Z}_n + (2w_0 - w_1)\mathcal{Z}_{n-1} + (w_1 - w_2)\mathcal{Z}_{n-2} + (w_2 - w_3)\mathcal{Z}_{n-3} + \cdots + (w_{k-1} - w_k)\mathcal{Z}_{n-k} = 0$$

which is a generalization of (3.10). It can be rewritten in compact form:

$$\mathcal{R}_{k+1}\mathcal{Z}_{n+1} = 0 \qquad n \geqslant k \tag{A.1}$$

if the linear operator

$$\mathcal{R}_{k+1} f_{n+1} \equiv f_{n+1} - (1 + 2w_0) f_n + (2w_0 - w_1) f_{n-1} + (w_1 - w_2) f_{n-2} + \cdots + (w_{k-1} - w_k) f_{n-k} \tag{A.2}$$

is introduced. Directly related to the operator $\mathcal{R}_{k+1}$ is the characteristic equation

$$P_{k+1}(\lambda) \equiv \lambda^{k+1} - (1 + 2w_0)\lambda^k + (2w_0 - w_1)\lambda^{k-1} + (w_1 - w_2)\lambda^{k-2} + \cdots + (w_{k-1} - w_k) = 0 \tag{A.3}$$

whose maximal root, $\lambda_{\rm max}$, from the set $\{\lambda_1, \ldots, \lambda_{k+1}\}$, determines the asymptotic behaviour of the partition function.

Analogous equations for the $\mathcal{D}^{(m)}$-functions can be derived and written in compact form as

$$\mathcal{R}_{k+1}\mathcal{D}^{(m)}_{n+1} = w_m(\mathcal{Z}_{n-m} - \mathcal{Z}_{n-m-1}) \tag{A.4}$$

where $2w_0$ must be substituted for w_m for $m = 0$.

In our formalism it is sufficient to find the $\mathcal{D}^{(m)}$-functions up to rank k ($m = 0, 1, \ldots, k$). For higher rank $m > k$ one obtains

$$\mathcal{D}^{(m)}_{n+m-k} = \mathcal{D}^{(k)}_n. \tag{A.5}$$

This relationship becomes clear from the form of equations (A.4) for $m \geqslant k$, where $w_m = w_k$.

An obvious *ansatz* for solving equations (A.1) is

$$\mathcal{Z}_n = \sum_{i=1}^{k+1} c_i \lambda_i^n \tag{A.6}$$

whereas for the solutions of equations (A.4) we use

$$\mathcal{D}_n^{(r)} = \sum_{i=1}^{k+1} (a_i^{(r)} + b_i^{(r)} n)\lambda_i^n \qquad r = 0, 1, \ldots, k. \tag{A.7}$$

We do not need the complete set of coefficients $\{a_i^{(r)}, b_i^{(r)}, c_i\}$, which can be calculated by using the boundary conditions, but rather the set of ratios $\{b_{\max}^{(m)}/c_{\max}\}$, which yields the concentrations x_m.

After inserting the *ansatz* (A.7) into equation (A.4), we compare the leading terms, which are given in terms of powers of $\lambda_{\max}$. Neglecting all other terms is equivalent to taking the thermodynamic limit. The basic result for the concentrations x_m reads

$$x_m = \frac{b_+^{(m)}}{c_+} = \frac{w_m(\lambda_{\max} - 1)\lambda_{\max}^{k-m-1}}{Q_{k+1}(\lambda_{\max})} \tag{A.8}$$

where

$$\begin{aligned} Q_{k+1}(\lambda) &= \lambda^{k+1} - (2w_0 - w_1)\lambda^{k-1} - 2(w_1 - w_2)\lambda^{k-2} - \cdots - k(w_{k-1} - w_k) \\ &\equiv \lambda^{k+1} \frac{\mathrm{d}}{\mathrm{d}\lambda}\left(\frac{P_{k+1}(\lambda)}{\lambda^k}\right). \end{aligned} \tag{A.9}$$

Combining equation (A.5) with result (A.8) yields

$$x_{k+m} = \frac{1}{\lambda_{\max}^m} x_k. \tag{A.10}$$

Appendix B

For the temperatures of interest we can write the susceptibility in the form

$$\begin{aligned} \chi = x_0\chi_0 + x_1\chi_1 + x_2\chi_2 + x_3(\chi_3 + \chi_4\lambda_{\max}^{-1} \\ + \chi_5(\lambda_{\max}^{-2} + \lambda_{\max}^{-3} + \cdots) + \chi'\lambda_{\max}^{-3}(1 + 2\lambda_{\max}^{-1} + 3\lambda_{\max}^{-2} + \cdots)). \end{aligned} \tag{B.1}$$

The most singular behaviour is contained in the term which is proportional to χ'. It can be accurately evaluated by using the sum rule (3.8). Let us reorganize the terms of (B.1) into three groups. The first one contains the non-singular contributions:

$$x_0\chi_0 + x_1\chi_1 + x_2\chi_2 + x_3(\chi_3 + \chi_4\lambda_{\max}^{-1} + \chi'\lambda_{\max}^{-3}(1 + 2\lambda_{\max}^{-1} + 3\lambda_{\max}^{-2})). \tag{B.2}$$

The second one is pseudo-singular:

$$\frac{x_3\chi_5}{\lambda_{\max}(\lambda_{\max} - 1)}. \tag{B.3}$$

Although the denominator in (B.3) vanishes if $\lambda_{\max} \to 1$, the complete term remains finite, since $x_3 \to 0$ in this limit, too (cf. equation (A.8).) Due to the sum rule

$$x_0 + 2x_1 + 3x_2 + x_3(4 + 5\lambda_{\max}^{-1} + 6\lambda_{\max}^{-2} + \cdots) = 1$$

the last contribution

$$x_3\chi'\lambda_{\max}^{-6}(4 + 5\lambda_{\max}^{-1} + 6\lambda_{\max}^{-2} + \cdots)$$

can be rewritten in the form

$$\chi'\lambda_{\max}^{-6}(1 - x_0 - 2x_1 - 3x_2) \tag{B.4}$$

which evidently approaches χ' when $\lambda_{\max} \to 1$.

References

[1] Niggemann H, Uimin G and Zittartz J 1997 *J. Phys.: Condens. Matter* **9** 9031 and references therein
[2] Boucher J P and Regnault L P 1996 *J. Physique* **6** 1939
[3] Garrett A W, Nagler S E, Tennant D A, Sales B C and Barnes T 1997 *Phys. Rev. Lett.* **79** 745
[4] Takahashi M 1989 *Phys. Rev.* B **40** 2494
[5] Klümper A 1992 *Ann. Phys., Lpz.* **1** 540
[6] Klümper A 1993 *Z. Phys.* B **91** 507